EurJIC European Journal of Inorganic Chemistry

ChemPubSoc Europe

FULL PAPER

DOI:10.1002/ejic.201500128

Syntheses, Spectroscopy, and Structural Analyses of Dinuclear Chiral-at-Metal μ-Aqua-tetrakis[(*R* or *S*)-*N*-1-(Ar)ethylsalicylaldiminato]di-Λ- or -Δ-nickel(II) Complexes

Mohammed Enamullah,*[a] Mohammad Abdul Quddus,[a] Mohammad Rezabul Hasan,[a] Gennaro Pescitelli,[b] Roberto Berardozzi,[b] Guido J. Reiß,[c] and Christoph Janiak*[c]

Keywords: Schiff bases / Nickel / Diastereoselectivity / Configuration determination / Enantioselectivity

Enantiopure dinuclear μ-aqua-tetrakis[(*R* or *S*)-*N*-1-(Ar)ethylsalicylaldiminato]di-Λ- or -Δ-nickel(II) [Ar = C_6H_5 (*R*-**1**/*S*-**1**), *p*-$MeOC_6H_4$ (*R*-**2**/*S*-**2**), *p*-ClC_6H_4 (*R*-**3**/*S*-**3**), *p*-BrC_6H_4 (*R*-**4**)] complexes have been synthesized from the reaction between (*R* or *S*)-*N*-1-(Ar)ethylsalicylaldimine and nickel(II) acetate. Their CD spectra demonstrate chirality transfer from the ligands to the metal ions and a mirror-image relationship for the enantiomeric pair *R*-**3**/*S*-**3** in thf. DSC analyses show that the complexes exhibit an irreversible dissociation to the mononuclear species, which in turn undergo decomposition. The ^{1}H NMR spectra reveal the presence of four salicylaldiminates, one aqua ligand, and two molecules of methanol in each dinuclear complex. They also confirm the existence of a dinuclear-bridged aqua bis-octahedral Ni^{II} complex in solution. The IR spectra in CH_2Cl_2 show a very strong band at around 2306 cm^{-1} due to the νO–H of the bridged aqua ligand. The X-ray structures of *R*-**2**, *S*-**2**, *R*-**3**, and *S*-**3** confirm the formation of dinuclear compounds comprising two nickel ions, four salicylaldiminates, and one aqua ligand with two molecules of methanol (or water in *S*-**2**). Each nickel ion is surrounded by two *N*,*O*-chelating salicylaldiminates, a bridging salicyl-O atom from the neighboring nickel ion, and a bridging aqua ligand in a distorted octahedral polyhedron. Analyses of the absolute structures reveal a diastereomeric induction of the *R* or *S* ligand giving a Λ or Δ configuration at the nickel atoms in *R*-**2**/**3** or *S*-**2**/**3** that is independent of the ligand substituents.

Introduction

Pseudo-octahedral six-coordinate tris- or bis-chelate Δ/Λ-metal complexes are classical textbook examples of metal-centered chirality. In these complexes, the asymmetry is due to the arrangement of an achiral or chiral ligand A^A(*) around a metal M, leading to D_3 symmetry for Δ/Λ-$M(A^A)_3$ or C_2 symmetry for Δ/Λ-$M(A^A)_2B_2$.[1–3] Use of enantiomeric chiral bidentate ligands leads to the formation of diastereomeric complexes with possible absolute configurations of Λ(*R*,*R*,*R*), Δ(*R*,*R*,*R*), Λ(*S*,*S*,*S*), or Δ(*S*,*S*,*S*).[4–9] If the chiral ligand is racemic, the mixed forms Λ(*R*,*S*,*S*) and Δ(*S*,*R*,*R*) etc. may also be obtained in addition. Moreover, in such chiral-at-metal complexes, the metal-centered configuration Δ or Λ (see Scheme 1) can be induced by the *R* or *S* chirality of the ligand.[2–4,6–13] Intramolecular noncovalent interactions acting within the chiral-at-metal chelate complexes lead to a free-energy difference between the diastereomers, and one of the diastereomers is generally dominant (termed stereochemical or diastereomeric induction). For example, the predominant formation of one diastereomer has been reported in a number of four-coordinate tetrahedral to distorted square-planar cases, including Λ-bis[(*R*)-*N*-(Ph)ethyl-X-Sal]Ni/Zn^{II} (Ph = phenyl; Sal = salicylaldiminato; X = H, 5-NO_2/OMe, 3,5-di-Cl),[6c,7a,7d] Δ-bis[(*R*)-*N*-(Ph)ethyl-X-Sal]Cu^{II} (X = 4-Br, 3,5-di-Cl),[6a,6b] Λ-bis[(*R*)-*N*-(Ph)ethyl-X-Sal]Cu^{II} (X = H, 3-OEt),[6b,6d] Δ-bis[*N*-(L-menthyl)-Sal]Co^{II},[7b] Δ-bis[(*R*)-*N*-(naphthyl)ethyl-3,5-di-Cl-Sal]Cu/Ni/Zn^{II},[7c] Δ-bis[AP-(*S*)-pn or AP-(*S*,*S*)-dpen]Ni^{II} (pn = enantiopure 1,2-diaminopropane; AP = 2-hydroxyacetophenone),[8] and Λ-bis[AP- or DA-(*S*,*S*)-chxn]Ni^{II} (DA = dehydroacetic acid),[8] as evidenced by solid-state crystal-structure determinations. Some analogous complexes have shown absolute configurations (Δ vs. Λ) based only on CD spectral patterns in solution.[5] In relation to this, some of us have reported an equilibrium of both Δ and Λ diastereomers with a diastereomeric ratio of around 20:80 in $CDCl_3$ for *R*,*R* ligands in Λ/Δ-configured bis[(*R*)-*N*-1-(Ar)ethylsalicylaldiminato-κ^2N,O]Zn^{II}, which compares with the enantiopure induc-

[a] Department of Chemistry, Jahangirnagar University, Dhaka 1342, Bangladesh
E-mail: enamullah@juniv.edu
http://people.juniv.edu/profile/enamullah
[b] Department of Chemistry, University of Pisa, via Moruzzi 3, 56124 Pisa, Italy
[c] Institut für Anorganische Chemie und Strukturchemie, Heinrich-Heine-Universität, Universitätsstr. 1, 40225 Düsseldorf, Germany
E-mail: janiak@uni-duesseldorf.de
http://www.janiak.hhu.de

Supporting information for this article is available on the WWW under http://dx.doi.org/10.1002/ejic.201500128.

tion of Λ(*R*,*R*) in the crystalline state.[9] Recently we reported a case of induced chirality-at-metal and diastereoselectivity for Δ/Λ-configured distorted square-planar Cu/Ni^{II} complexes by enantiopure (*R* or *S*)-*N*-1-(Ar)ethylnaphthaldimine/salicylaldimine ligands (Ar = C_6H_5, *m*/*p*-$MeOC_6H_4$, and *p*-Cl/BrC_6H_4) on the basis of combined CD, DFT, and X-ray structural analyses both in solution and the solid state.[12,13] We have also reported the syntheses, stereochemistry, and diastereoselectivity of Λ/Δ-configured distorted tetrahedral zinc(II) and copper(II) complexes with enantiopure or racemic amino alcohol based Schiff base ligands.[14,15] Here, the *N*,*O*-chelation of two enantiopure or racemic ligands to four-coordinate, nonplanar Zn(*R*/*S*-N^O)$_2$ leads to the preferential formation of one diastereomer in a ratio of around 67:33 for Λ-Zn-*R*/Δ-Zn-*R* (or Δ-Zn-*S*/Λ-Zn-*S*) in solution or the racemate of the enantiomeric pair Λ-Zn-*S* and Δ-Zn-*R* in the solid state.[14]

In a similar way, induced diastereoselection (Δ vs. Λ) by a chiral bi- or tridentate chelate ligand at the metal center in a six-coordinate octahedron has proved to be of considerable interest.[1–4,16–18] In fact, the stereoselective synthesis of $[Pt(pn)_2Cl_2]^{2+}$ and $[Pt(pn)_3]^{4+}$ was first reported by Smirnoff,[16a] based on optical rotation in solution. This phenomenon has also been observed in bridged dinuclear octahedral complexes using suitable chiral building blocks in the solid state.[2a,2b,4] A pronounced diastereoselectivity was reported in dinuclear ΔΔ[Rh(L)$_2$(μ-Cl)]$_2$ [L = th4,5(*R*,*R*)ppy] with ΔΔ/ΛΛ = 9:1 and in ΛΛ[Rh(L′)$_2$(μ-Cl)]$_2$ [L′ = th4,5(*S*,*S*)ppy] with ΛΛ/ΔΔ = 9:1, according to the results of X-ray studies.[17a]

However, the reported examples of induced diastereoselection in Ni^{II} chiral-*N*,*O*-chelate complexes are limited to mononuclear four-coordinate tetrahedral to distorted square-planar geometries.[7c,8,13] Although two examples of six-coordinate dinuclear μ-aqua-bis[*N*-(Ar)-5-nitrosalicylaldiminato]dinickel(II)[19] complexes are available, no such diastereoselection in octahedral mono- or dinuclear Ni^{II} (*R* or *S*)-*N*,*O*-chelate complexes has been reported in either the solid state or in solution. Thus, dinuclear nickel(II) (*R* or *S*)-*N*,*O*-chelate complexes are of continued interest in the field of diastereoselection phenomena, especially with the aim to evidence correlations between the absolute configurations (Δ vs. Λ) in the solid state and CD spectral patterns in solution. This paper reports, for the first time, distorted octahedral dinuclear μ-aqua-tetrakis[(*R* or *S*)-*N*-1-(Ar)ethylsalicylaldiminato]di-Λ- or -Δ-nickel(II) complexes with diastereomeric induction at the metal center (Δ vs. Λ configurations) by *R* or *S* ligand chirality. The ligand substituents are also taken into account to affect the phenomena, if any.

Results and Discussion

The enantiopure Schiff base ligands (*R* or *S*)-*N*-1-(Ar)-ethylsalicylaldimine (HL) were treated with nickel(II) acetate to give enantiopure dinuclear μ-aqua-tetrakis[(*R* or *S*)-*N*-1-(Ar)ethylsalicylaldiminato]di-Λ- or -Δ-nickel(II) complexes [Ar = C_6H_5 (*R*-**1** or *S*-**1**), *p*-$MeOC_6H_4$ (*R*-**2** or *S*-**2**), *p*-ClC_6H_4 (*R*-**3** or *S*-**3**), and *p*-BrC_6H_4 (*R*-**4**); Scheme 1].

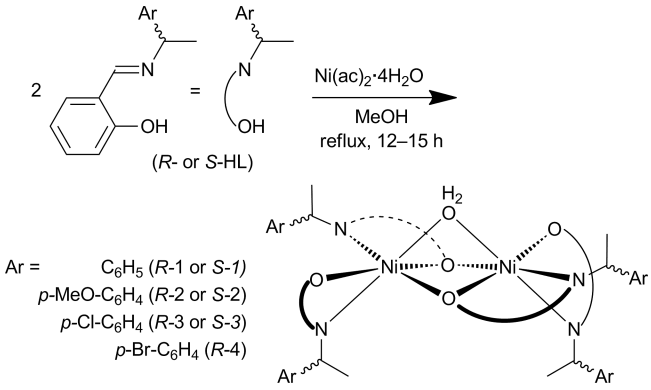

Scheme 1. Synthetic route to dinuclear μ-aqua-tetrakis[(*R* or *S*)-*N*-1-(Ar)ethylsalicylaldiminato]di-Λ- or -Δ-nickel(II). The drawing of the dinuclear nickel complex depicts the Δ configuration at both nickel atoms, as found for ***S*-2** and ***S*-3** with the *S* ligand.

Vibrational Spectra

The main characteristic bands observed in the IR spectra, recorded as KBr discs, are listed in Table S1 in the Supporting Information. A very strong νC=N band is observed at 1627–1599 cm^{-1} for the imine group,[20–25] and weak bands are observed at around 3634 cm^{-1} due to the νO–H of methanol (crystal solvent) and at around 2375 and 2360 cm^{-1} due to the νO–H of the bridged aqua ligand.[24] Several bands/shoulders are also observed at around 3250, 3085–2930, and 1589–1577 cm^{-1}, associated with νH_2O (from KBr), νC–H, and νC=C, respectively. To confirm the existence of the dinuclear-bridged aqua Ni^{II} complexes in solution, we recorded the IR spectra of *R*-**3** and *R*-**4** in dichloromethane (see Figure S1 and Table S1). The spectra of the compounds are identical and similar to those recorded in KBr discs, except for the presence of a very strong band at around 2306 cm^{-1} due to the νO–H of the bridging aqua ligand, as confirmed by the deuterium isotope shift.[24a] The spectra in DCM also show a medium band at around 3945 cm^{-1} and two weak bands at around 3755 and 3692 cm^{-1} due to two molecules of methanol in the crystals.[24b] Thus, the IR data confirm the existence of dinuclear bridged aqua Ni^{II} complexes in solution.

Mass Spectra

The EI mass spectra of **1**–**4** (see Figures S2 and S3 and Table S2) show ion peaks at *m*/*z* = 506 (**1**), 566 (**2**), 576 (**3**), and 664 (**4**), corresponding to the mononuclear species $[Ni(L)_2]^+$. The peaks at *m*/*z* = 562 (**1**), 632 (**3**), and 722 (**4**) correspond to the dinuclear monoligated $[(NiL - H)_2]^+$ species. The peaks at *m*/*z* = 281/283 (**1**), 311/313 (**2**), 315/317 (**3**), and 361/363 (**4**) are associated with the two monoligated $[NiL - H]^+$/$[NiL + H]^+$ species. The spectra are also dominated by several peaks arising from the Schiff bases (HL) and fragmented Schiff bases. The CI(NH_3) mass spec-

tra (see Figures S2 and S3 in the Supporting Information) show ion peaks at m/z = 507 (**1**) and 567 (**2**) for the protonated mononuclear $[Ni(L)_2 + H]^+$ species as well as peaks for $[NiL + H]^+$ and $[HL + H]^+$ species. Indeed, the ESI (positive) mass spectra show no ion peak for the μ-aquadinuclear species, except for the protonated Schiff base ligands ($[HL + H]^+$) in solution.

Polarimetry

Polarimetric measurements show rotations to the right or left with $[\alpha]_D$ values of +312.5 or –307.2° (*R*-**1** or *S*-**1**), +350.9 or –357.1° (*R*-**2** or *S*-**2**), +367.5 or –375.0° (*R*-**3** or *S*-**3**), and +392.9° (*R*-**4**) (Table S3), thereby confirming the enantiopurity or very similar enantiomeric excesses of the complexes in chloroform solution.

DSC Analyses

Differential scanning calorimetry (DSC) analyses show that the free Schiff base ligand undergoes reversible phase transformation from the crystalline to the isotropic liquid phase, as evidenced in both the first and second cycles of the heating/cooling curves (Figure 1, left, Table 1).[12,15,18] On the other hand, all the complexes show a broad exothermic peak below 100 °C (Figure 1, right, for *R*-**2** and *R*-**3**), corresponding to an irreversible dissociation and formation of the mononuclear species. On further heating, a second exothermic peak can be seen at 104 (*R*-**2**) and 113 °C (*R*-**3**), corresponding to an irreversible decomposition of the mononuclear species.

Table 1. DSC analyses data for the compounds.

Entity	Peak [°C]/Δ*H* [kJ mol^{-1}]	
	Heating	Cooling
HL1	75/–23.93 (74/–21.58)[a]	51/+21.40 (50/+20.58)[a]
R-**1**	56	no peak
R-**2**	68, 104/–3.55	no peak
R-**3**	81, 113/–15.25	no peak
R-**4**	84	no peak

[a] The values in parentheses are for the second heating/cooling cycle.

Electronic Spectra

Absorption and CD spectra were recorded for compounds *R*-**1**, *R*-**2**, *R*-**3**, and *S*-**3** in anhydrous thf solution in the range 200–800 nm (Figures 2–4). All the absorption spectra are similar to each other. The spectra show a weak band at around 420 nm, a moderately intense band between 310 and 360 nm, and three intense bands below 300 nm (270, 240, and 220 nm; this last band is absent for *R*-**1**). The

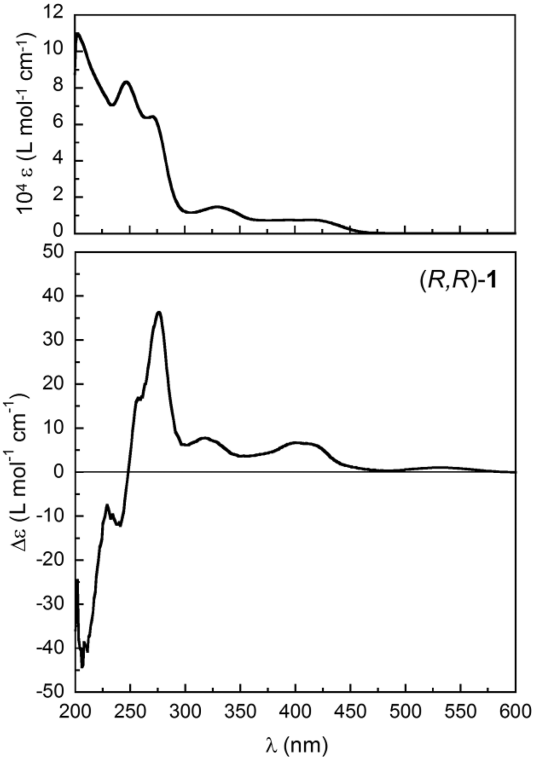

Figure 2. UV/Vis (top) and CD spectra (bottom) of *R*-**1** in thf (1.09 mM; cell path-length: 0.1 mm, 200–300 nm; 5 mm, 300–500 nm; 10 mm, 500–600 nm).

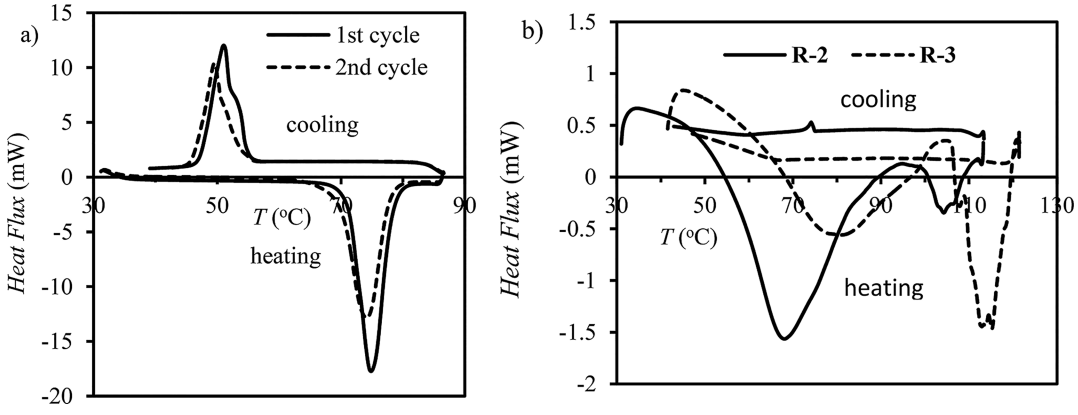

Figure 1. DSC analyses curves of (a) the Schiff base (**HL1**) and (b) ***R*-2** and ***R*-3**.

bands associated with metal transitions (see below) are not detectable in the absorption spectra due to their weakness, allied with a substantial electric–dipole forbidden character. With the exception of the band at 220 nm, the positions and relative intensities of the other bands are well preserved among all the spectra.

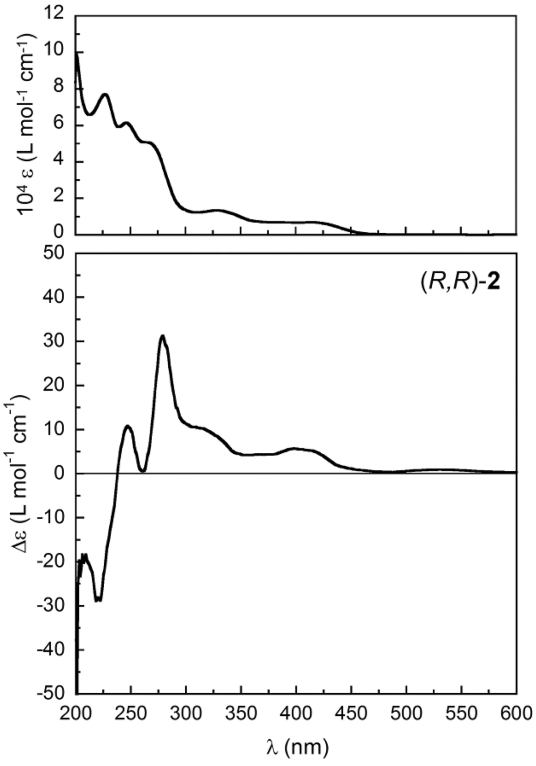

Figure 3. UV/Vis (top) and CD spectra (bottom) of *R*-**2** in thf (1.98 mM; cell path-length: 0.1 mm, 200–300 nm; 5 mm, 300–500 nm; 10 mm, 500–600 nm).

Similarly to the absorption spectra, the CD spectra show several common features. The CD spectra of the enantiomeric compounds *R*-**3** and *S*-**3** are the mirror image of each other (Figure 4). All the complexes with the *R*,*R* ligand configuration (*R*-**1**, *R*-**2**, and *R*-**3**) show one weak positive band in the visible range at around 530 nm and a medium-intense positive band in the range 360–440 nm. There are three bands at shorter wavelengths: A positive band at 300–330 nm, which in some cases appears as a shoulder of a more intense and structured band with a positive sign in the range 260–300 nm, flanked by a strong negative band at around 230–270 nm. The intensity and position of the most intense band depends on the compound; for *R*-**2**, we observe a blueshift for this band and the presence of an additional band at 250 nm.

Summarizing, the Ni complexes are characterized by the following CD bands, which are indicative of the *R*,*R* ligand configuration [approximate band wavelength (sign, and strength)]: 530 nm (+, weak), 410 nm (+, medium), 320 nm (+, medium), 275 nm (+, strong), and 245 nm (–, strong). In the solid-state structure determinations, the *R*,*R* ligand configuration corresponds selectively to the Λ configuration at the nickel atoms (see below).

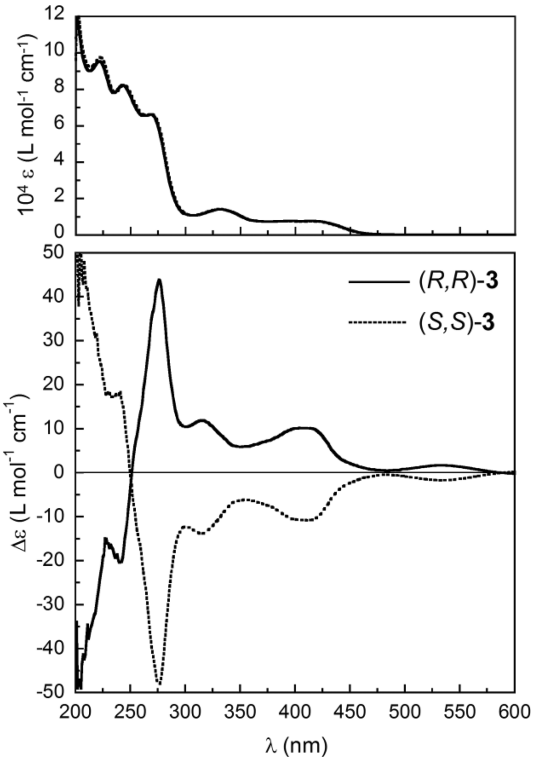

Figure 4. UV/Vis (top) and CD spectra (bottom) of *R*-**3** and *S*-**3** in thf (1.71 and 1.33 mM, respectively; cell path-length: 0.1 mm, 200–300 nm; 5 mm, 300–500 nm; 10 mm, 500–600 nm).

Molecular orbital and transition analyses, carried out by means of DFT calculations at the B3LYP/TZVP level of theory, allowed the band at around 530 nm to be attributed to metal-centered d–d transitions with some metal-to-ligand (M–L) charge-transfer character, the band at 410 nm is a combination of d–d and M–L charge transfer with the π–π* transition (^1L_b type) on the salicylaldiminato ring, the band at 320 nm arises mainly from two π–π* transitions (^1L_b and ^1L_a type) on the salicylaldiminato ring, and the bands at higher energies arise from the superposition of several different transitions, mostly located on the aromatic rings of the ligands. Generally speaking, however, a clear separation between metal- and ligand-centered transitions is impossible because several metal-centered transitions occur also in the UV region of the spectrum.

^{1}H NMR Spectroscopy

The ^{1}H NMR spectra of the compounds in $CDCl_3$ (green solutions) show several broad peaks associated with the Schiff base ligands coordinated to a paramagnetic nickel ion (Figure 5, Table 2). The coordinated aqua ligand and crystal solvent (methanol) show broad peaks at δ = 3.50–3.65 and 3.70–3.90 ppm, respectively. The spectra also show peaks due to the presence of a small amount of the free Schiff base ligand in the samples (see asterisked peaks in Figure 5), in good agreement with reported spectra.[20] The integration reveals the presence of four deprotonated Schiff base ligands, one aqua ligand, and two molecules of meth-

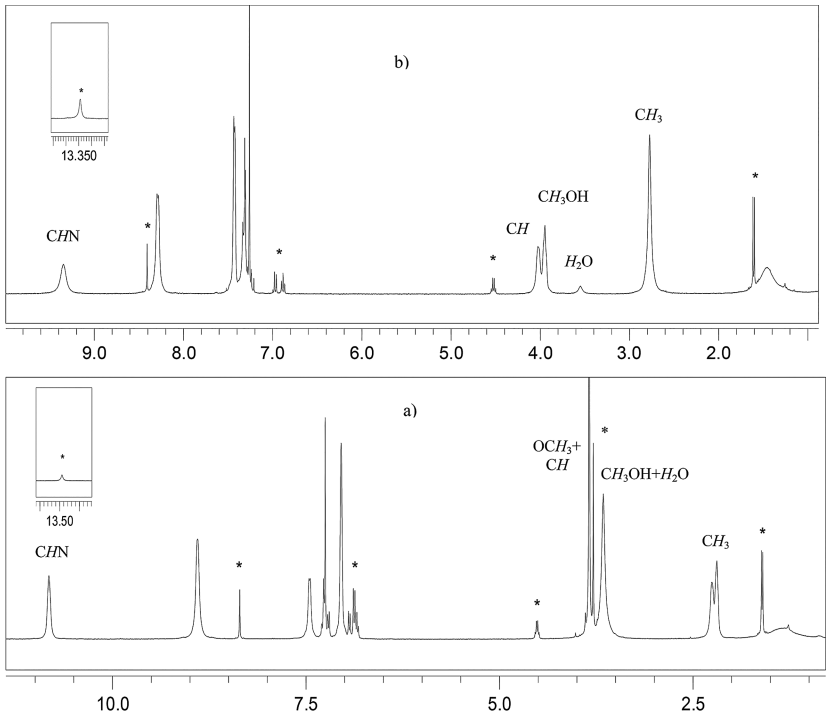

Figure 5. ^{1}H NMR (400 MHz) spectra of (a) ***R*-2** and (b) ***R*-3** in $CDCl_3$ at 20 °C (asterisked peaks correspond to the free Schiff base ligand in the sample).

Table 2. ^{1}H NMR (400 MHz) data of the complexes in $CDCl_3$ at 20 °C.[a]

Entity	CH_3	H_2O	CH_3OH	OCH_3	CH	Ar–H	CHN
R-**1**	2.88 (12 H)	3.50 (2 H)	3.80 (6 H)	–	3.89 (4 H)	7.40 (12 H), 7.50 (12 H), 8.42 (12 H)	9.44 (4 H)
R-**2**	2.22 (12 H)	3.66 (2 H)	3.66 (6 H)	3.84 (12 H)	3.86 (4 H)	7.04 (10 H), 7.26 (6 H), 7.45 (6 H), 8.90 (10 H)	10.82 (4 H)
R-**2**[b]	1.40 (d, *J* = 6.6 Hz, 12 H)	3.15 (2 H)	3.73 (6 H)	3.71 (s, 12 H)	4.33 (q, *J* = 6.6 Hz, 4 H)	6.01 (t, *J* = 7.4 Hz, 4 H), 6.28 (d, *J* = 8.4 Hz, 4 H), 6.86 (d, *J* = 8.8 Hz, 12 H), 7.29 (d, *J* = 8.7 Hz, 8 H), 7.44 (d, *J* = 7.8 Hz, 4 H)	8.71 (s, 4 H)
R-**3**	2.77 (12 H)	3.55 (2 H)	3.95 (6 H)	–	4.03 (4 H)	7.26 (6 H), 7.31 (6 H), 7.43 (10 H), 8.28 (10 H)	9.35 (4 H)
R-**4**	2.85 (12 H)		3.90 (6 H)	–	4.01 (4 H)	7.26 (8 H), 7.52 (8 H), 7.62 (8 H), 8.28 (8 H)	9.36 (4 H)
R-**4**[b]	1.42 (d, *J* = 6.6 Hz, 12 H)	3.43 (2 H)	3.43 (6 H)	–	4.36 (q, *J* = 6.6 Hz, 4 H)	5.97 (t, *J* = 7.3 Hz, 4 H), 6.21 (d, *J* = 7.7 Hz, 4 H), 6.84 (t, *J* = 7.8 Hz, 4 H), 7.35 (m, 12 H), 7.51 (d, *J* = 8.0 Hz, 8 H)	8.68 (s, 4 H)

[a] Asterisked peaks for the free Schiff base ligands are not listed. [b] Spectrum recorded in the presence of KCN in $[D_6]$DMSO at 20 °C.

anol in each dinuclear Ni^{II} complex. The compound dissociates in the presence of KCN in $[D_6]$DMSO with the formation of diamagnetic $[Ni(CN)_4]^{2-}$ to give a light-yellow solution.[12,25a] The spectra of the reaction mixtures of *R*-**2** and *R*-**4** (Figure 6, Table 2) show similar results with sharp peaks arising from the deprotonated Schiff base ligands, water (both from the complex and $[D_6]$DMSO), and methanol.

To confirm the existence of dinuclear bridged aqua Ni^{II} complexes in solution, we analyzed the spectra (Figure 5, Table 2) and found that there is little difference in the chemical shifts between the complex and free-ligand peaks, despite there being some broadening of the peaks of the Ni^{II} complexes. A mononuclear Ni^{II} complex with a square-planar structure would be diamagnetic and would show no signal broadening, hence, this structure can be excluded. Furthermore, a mononuclear Ni^{II} complex with a tetrahedral structure would show pronounced differences in the chemical shifts of several ppm with respect to the free ligand peaks and hence this structure can also be excluded. Therefore we can conclude the existence of dinuclear bridged aqua bis-octahedral Ni^{II} complexes in solution with two not fully antiferromagnetically coupled nickel ions, matching well the experimental ^{1}H NMR spectra.

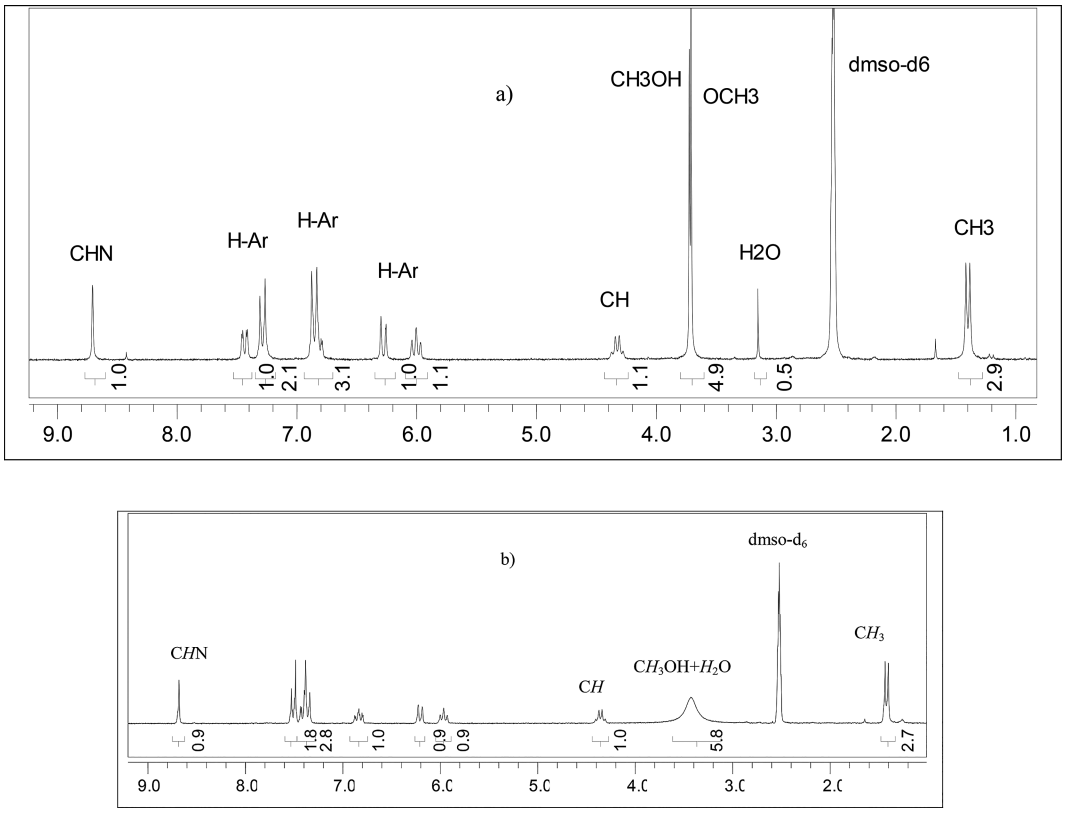

Figure 6. ^{1}H NMR (400 MHz) spectra of (a) ***R*-2** and (b) ***R*-4** in the presence of KCN in [D$_6$]DMSO at 20 °C.

Solid-State Structures

Crystals of complexes **2** and **3**, suitable for single-crystal X-ray studies, were grown from concentrated solutions in methanol. The chiral compounds crystallize in the noncentrosymmetric monoclinic space group *C*2. The X-ray data of all four compounds are in agreement with the formation of dinuclear complexes with two nickel ions, four salicylaldiminato ligands, and an aqua ligand (Scheme 1, Figure 7, Table 3). Two molecules of methanol in *R*-**2**, *R*-**3**, and *S*-**3** and two molecules of crystal water in *S*-**2** complement the crystal packing of each dinuclear unit. Each Ni ion is surrounded by two *N*,*O*-chelating Schiff base ligands, a bridging salicyl-O atom from the neighboring nickel ion, and a bridging aqua ligand in a distorted octahedral polyhedron. Thus, the dinuclear unit is constructed of two face-sharing octahedra. The triatomic bridge is formed from salicyl-O atoms and the O atom of the aqua ligand.

The two Schiff base ligands around the Ni atom are not equal: One is chelating only (-κ^2*N*,*O*) whereas the other is chelating and bridges the two Ni atoms through its salicyl-O atom (-κ^3*N*,*O*:*O*). Hence, the name of the dinuclear complex would be μ-aqua-bis[(*R* or *S*)-*N*-1-(Ar)ethylsalicylaldiminato-κ^2*N*,*O*]-bis[(*R* or *S*)-*N*-1-(Ar)ethylsalicylaldiminato-κ^3*N*,*O*:*O*]di-Λ- or -Δ-nickel(II).

The two planes of the six-membered metal–Schiff base chelate rings give rise to metal-centered chirality with a bischelate Δ/Λ configuration of a pseudo-octahedral six-coordinate Δ/Λ-Ni(N^O)$_2$O$_2$ unit.[1,19] The dinuclear complex is located in a special position with the C_2 axis passing through the aqua ligand and the center of the Ni···Ni connector. Thus, the two halves of the dinuclear complex are C_2-symmetry related. Hence, by symmetry, both Ni atoms must be of the same Λ or Δ configuration. Analyses of the absolute structures of the crystals reveal that the diastereomeric induction of the *R* ligands in compounds *R*-**2** and *R*-**3** give the Λ configuration and the *S* ligands in compounds *S*-**2** and *S*-**3** yield the Δ configuration at the nickel atoms. However, this diastereomeric induction does not depend on the substituents on the aromatic ring of the ligand. Thus, the diastereomeric induction is similar to that in Λ/Δ-Zn-(*R* or *S*)-*N*,*O*-chelates[9] and different to that in Λ/Δ-Cu/Ni-(*R* or *S*)-*N*,*O*-chelates,[6a,6b,8,12,13] in which ligand substituents seem to play a vital role in the phenomena.

From the absolute structure (Flack) parameters,[26] which are between –0.002 and –0.034 (see Table 4), the crystals of complexes **2** and **3** appear to be enantio- and diastereopure. A Flack parameter (x) close to zero within an uncertainty (u) of <0.04 and with $|x|$ within $3u$, that is, $|x|/u < 3$, confirms the correct absolute structure[27] and, together with the other refinement parameters, rules out the presence of significant amounts of opposite metal chirality within the investigated crystal. The existence of the other diastereomer after the formation of a diastereomeric conglomerate cannot be precluded on the basis of data from single-crystal experiments alone. We note, however, that for each complex the corresponding opposite stereochemical induction was

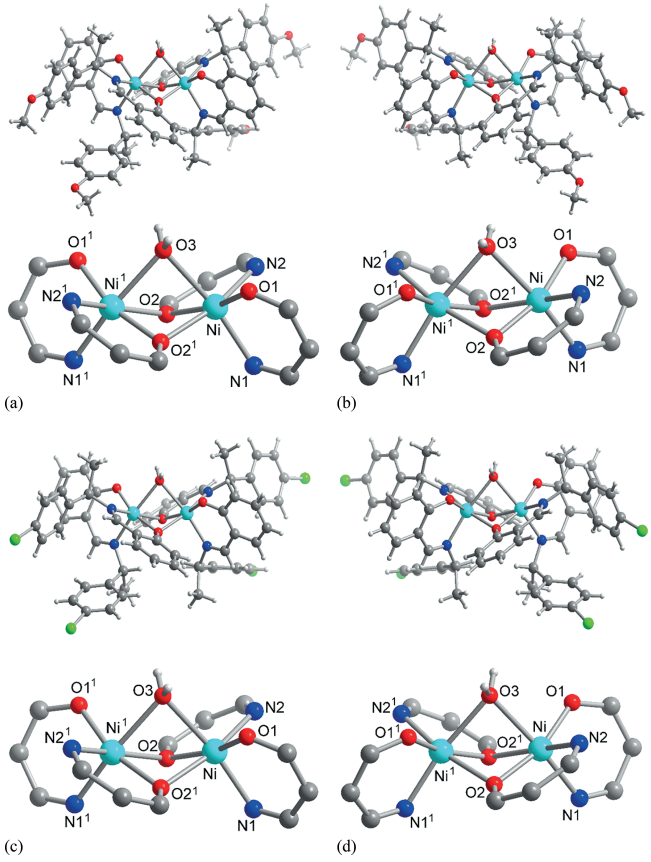

Figure 7. Full molecular structures and the metal–chelate ring cores of **2** and **3** for (a) *R*-**2** with the (*R*)-Λ configuration, (b) *S*-**2** with (*S*)-Δ, (c) *R*-**3** with (*R*)-Λ, and (d) *S*-**3** with (*S*)-Δ. Symmetry transformation: 1 = –*x* + 1, *y*, –*z* in *R*-**2** and *R*-**3**; –*x* + 1, *y*, –*z* + 2 in *S*-**2** and *S*-**3**. The disorder of the methoxy group in *R*-**2** and ***S*-2** and the crystal solvent molecules in all structures are not shown for clarity.

observed for the two pairs of enantiomeric ligands, which makes this possibility very improbable.

Conclusions

The reaction of enantiopure (*R* or *S*)-*N*-1-(Ar)ethylsalicylaldimine with nickel(II) acetate provides dinuclear μ-aqua-tetrakis[(*R* or *S*)-*N*-1-(Ar)ethylsalicylaldiminato]di-Λ- or -Δ-nickel(II) complexes. The CD spectra of *R*-**3** and *S*-**3** exhibit the expected mirror-image relationship of an enantiomeric couple. DSC analyses show the compound to exhibit irreversible dissociation to the mononuclear species, which subsequently undergo decomposition. Both the IR and ^{1}H NMR spectra confirm the existence of dinuclear bridged aqua bis-octahedral Ni^{II} complexes in solution. Molecular structure determinations show that each nickel ion is surrounded by two salicylaldiminates, one bridging salicyl-O atom from the neighboring nickel ion, and one bridging aqua ligand in a distorted octahedral polyhedron. Analyses of the absolute structures demonstrate diastereoselective induction-at-nickel by the *R* or *S* ligands to give the Λ or Δ configuration in the complexes *R*-**2/3** and *S*-**2/3**. The results explore the induced chirality at the metal ion (Λ vs. Δ) in distorted bis-octahedral dinuclear μ-aqua-Ni^{II}-*N*,*O*-chelate complexes, efficiently controlled by the *R* or *S* ligand chirality, irrespective of the ligand substituents.

Experimental Section

Materials and Methods: FTIR spectra were recorded with a Nicolet iS10 (Thermo Scientific) spectrometer as KBr discs at ambient temperature. Elemental analyses were performed with a Vario EL instrument from Elementar Analysensysteme GmbH. Polarimetric measurements were carried with a Perkin–Elmer 241 polarimeter in $CHCl_3$ at 589 nm and 20 °C. Thermal analyses were performed with a Shimadzu DSC-60 differential scanning calorimeter in the heating range 303–395 K and at a rate of 10 K min^{-1}. ^{1}H NMR spectra were recorded with a Bruker Avance DPX 400 spectrometer operating at 400 MHz (^{1}H) in $CDCl_3$ or [D_6]DMSO at 20 °C. EI and CI (NH_3) mass spectra were recorded with a Thermo-Finnigan TSQ 700 spectrometer. ESI (positive) mass spectra were recorded in methanol/water solution. Isotopic distribution patterns arising from the ions containing $^{58/60}$Ni, $^{35/37}$Cl, or $^{79/81}$Br are clearly visible in the mass spectra. UV/Vis spectra were recorded with a Jasco V-650 spectrophotometer in thf at 20 °C. ECD spectra were obtained with a JASCO Spectropolarimeter (J715) in anhydrous thf with 1–2 mM samples. For each solution sample, three distinct spectra were recorded by using cells of different path lengths (0.1, 5, and 10 mm) to cover the whole spectral range from 200 to 800 nm by keeping the absorbance below 1.5 a.u. The enantiopure Schiff bases (*R* or *S*)-*N*-1-(Ar)ethylsalicylaldimine (*R*- or *S*-HL) were synthesized as described previously.[20–22]

General Procedure for the Synthesis of the Complexes: Enantiopure (*R* or *S*)-*N*-1-(C_6H_5)ethylsalicylaldimine (*R*- or *S*-**HL1**; 284 mg, 1.26 mmol) was dissolved in methanol (5 mL). This solution was poured into a methanolic solution (5 mL) of $Ni(O_2CCH_3)_2{\cdot}4H_2O$ (156 mg, 0.63 mmol) and heated at reflux with stirring for 12–15 h. The color of the solution changed from yellow to light green and finally to deep green. The solvent was evaporated to 50% volume and the remaining solution left to stand for crystallization at room temp. Bright-green crystals suitable for X-ray determination were formed after 4–5 d, removed by filtration, and washed three times with methanol. The crystals were then dried in air and obtained as bright-green crystals of μ-aqua-tetrakis[(*R* or *S*)-*N*-1-(phenyl)-ethylsalicylaldiminato]dinickel(II) (*R*-**1** or *S*-**1**). The same procedure was followed for the syntheses of μ-aqua-tetrakis[(*R* or *S*)-*N*-1-(Ar)ethylsalicylaldiminato]dinickel(II) {Ar = *p*-MeO-C_6H_4 (*R*-**2** or *S*-**2**), *p*-ClC_6H_4 (*R*-**3** or *S*-**3**), and *p*-BrC_6H_4 (*R*-**4**)} by using the Schiff bases (*R* or *S*)-*N*-1-(Ar)ethylsalicylaldimine (Ar = *p*-Me-OC_6H_4, *p*-ClC_6H_4, and *p*-BrC_6H_4), respectively.

μ-Aqua-tetrakis[(*R*)-*N*-1-(phenyl)ethylsalicylaldiminato]dinickel(II) (*R*-1): Yield 250 mg (72%). [α]^{25} (*c* = 0.05 g/100 mL, $CHCl_3$): + 312.5° (589 nm). MS (EI, 70 eV): *m*/*z* (%) = 562 (3) [$(NiL1 – H)_2$]$^+$, 506 (50) [M]$^+$, 356 (12) [{$C_6H_4(O)(CH{=}NH)Ni$}$_2$]$^+$, 283/281 (98:62) [NiL1 + H]$^+$/[NiL1 – H]$^+$, 225/224 (50:70) [HL1]$^+$/[HL1 – H]$^+$, 179 (85) [$C_6H_4(CH{=}NH)ONi$ + H]$^+$, 121 (30) [$CH(C_6H_5)(CH_3)$-(NH_2)]$^+$, 105 (100) [$CH(C_6H_5)(CH_3)$]$^+$ (M = $C_{30}H_{28}N_2O_2Ni$, HL1 = $C_{15}H_{15}NO$). $C_{60}H_{56}N_4O_4Ni_2$(μ-H_2O)·2CH_3OH (1096.65): calcd. C 67.91, H 6.07, N 5.11; found C 68.80, H 5.69, N 5.17.

μ-Aqua-tetrakis[(*S*)-*N*-1-(phenyl)ethylsalicylaldiminato]dinickel(II) (*S*-1): Yield 250 mg (72%). [α]^{25} (*c* = 0.04 g/100 mL, $CHCl_3$): –307.2° (589 nm). MS (EI, 70 eV): *m*/*z* (%) = 562 (3) [$(NiL1 – H)_2$]$^+$, 506 (55) [M]$^+$, 356 (10) [{$C_6H_4(O)(CH{=}NH)Ni$}$_2$]$^+$, 283/281

Table 3. Selected bond lengths [Å] and angles [°] in the compounds.

		R-**2**[a]				*S*-**2**[b]	
Ni–O1	1.982(2)	O1–Ni–O2	164.03(9)	Ni–O1	1.972(3)	O1–Ni–O2	164.20(11)
Ni–O2	2.008(2)	O1–Ni–N1	91.33(11)	Ni–O2	2.009(2)	O1–Ni–N1	91.28(13)
Ni–N1	2.038(3)	O2–Ni–N1	101.80(11)	Ni–N1	2.036(3)	O2–Ni–N1	101.61(13)
Ni–N2	2.063(3)	O1–Ni–N2	97.15(11)	Ni–N2	2.057(3)	O1–Ni–N2	97.25(13)
Ni–O2^1	2.131(2)	O2–Ni–N2	90.83(10)	Ni–O2^1	2.129(2)	O2–Ni–N2	90.76(12)
Ni–O3	2.281(3)	N1–Ni–N2	94.81(12)	Ni–O3	2.284(4)	N1–Ni–N2	94.91(14)
Ni–Ni^1	2.9874(7)	O–Ni–O2^1	93.79(9)	Ni–Ni^1	2.9863(7)	O1–Ni–O2^1	93.73(11)
O3–Ni^1	2.281(3)	O2–Ni–O2^1	76.50(9)	O3–Ni^1	2.284(4)	O2–Ni–O2^1	76.54(11)
O3–H3	0.750(5)	N1–Ni–O2^1	93.69(10)	O3–H3	0.730(5)	N1–Ni–O2^1	93.66(12)
		N2–Ni–O2^1	165.97(10)			N2–Ni–O2^1	165.90(12)
		O1–Ni–O3	87.91(9)			O1–Ni–O3	88.14(10)
		O2–Ni–O3	77.41(9)			O2–Ni–O3	77.42(10)
		N1–Ni–O3	168.64(9)			N1–Ni–O3	168.71(11)
		N2–Ni–O3	96.53(10)			N2–Ni–O3	96.35(12)
		O2^1–Ni–O3	75.06(8)			O2^1–Ni–O3	75.14(10)
		O1–Ni–Ni^1	119.35(7)			O1–Ni–Ni^1	119.52(8)
		O2–Ni–Ni^1	45.46(6)			O2–Ni–Ni^1	45.42(7)
		N1–Ni–Ni^1	122.66(8)			N1–Ni–Ni^1	122.51(9)
		N2–Ni–Ni^1	123.96(8)			N2–Ni–Ni^1	123.83(10)
		O2^1–Ni–Ni^1	42.18(6)			O2^1–Ni–Ni^1	42.22(7)
		O3–Ni–Ni^1	49.09(7)			O3–Ni–Ni^1	49.18(8)
		Ni^1–O3–Ni	81.82(14)			Ni–O3–Ni^1	81.64(17)
		Ni^1–O3–H3	111(5)			Ni–O3–H3	120(6)
		Ni–O3–H3	127(5)			Ni^1–O3–H3	102(6)
		R-**3**[a]				*S*-**3**[b]	
Ni–O1	1.977(18)	O1–Ni–O2	163.84(7)	Ni–O1	1.976(16)	O1–Ni–O2	163.87(7)
Ni–O2	2.011(17)	O1–Ni–N1	91.61(8)	Ni–O2	2.010(15)	O1–Ni–N1	91.40(7)
Ni–N1	2.038(2)	O2–Ni–N1	101.75(8)	Ni–N1	2.039(19)	O2–Ni–N1	101.96(7)
Ni–N2	2.056(2)	O1–Ni–N2	96.93(8)	Ni–N2	2.056(19)	O1–Ni–N2	96.87(8)
Ni–O2^1	2.129(17)	O2–Ni–N2	91.22(8)	Ni–O2^1	2.129(15)	O2–Ni–N2	91.26(7)
Ni–O3	2.276(2)	N1–Ni–N2	94.06(9)	Ni–O3	2.276(2)	N1–Ni–N2	93.85(8)
Ni–Ni^1	2.9780(6)	O1–Ni–O2^1	93.84(7)	Ni–Ni^1	2.9777(6)	O1–Ni–O2^1	93.85(6)
O3–Ni^1	2.276(2)	O2–Ni–O2^1	76.46(8)	O3–Ni^1	2.276(2)	O2–Ni–O2^1	76.47(7)
O3–H3	0.840(3)	N1–Ni–O2^1	93.58(8)	O3–H3	0.840(3)	N1–Ni–O2^1	93.75(7)
		N2–Ni–O2^1	166.61(7)			N2–Ni–O2^1	166.69(7)
		O1–Ni–O3	87.33(6)			O1–Ni–O3	87.37(6)
		O2–Ni–O3	77.82(6)			O2–Ni–O3	77.79(6)
		N1–Ni–O3	168.94(7)			N1–Ni–O3	169.05(6)
		N2–Ni–O3	96.99(7)			N2–Ni–O3	97.10(6)
		O2^1–Ni–O3	75.52(6)			O2^1–Ni–O3	75.49(6)
		O1–Ni–Ni^1	119.00(5)			O1–Ni–Ni^1	119.05(5)
		O2–Ni–Ni^1	45.63(5)			O2–Ni–Ni^1	45.61(4)
		N1–Ni–Ni^1	123.06(6)			N1–Ni–Ni^1	123.26(5)
		N2–Ni–Ni^1	124.44(6)			N2–Ni–Ni^1	124.55(6)
		O2^1–Ni–Ni^1	42.45(5)			O2^1–Ni–Ni^1	42.43(4)
		O3–Ni–Ni^1	49.14(5)			O3–Ni–Ni^1	49.14(4)
		Ni^1–O3–Ni	81.72(10)			Ni–O3–Ni^1	81.72(9)
		Ni^1–O3–H3	108(3)			Ni–O3–H3	123(3)
		Ni–O3–H3	123(3)			Ni^1–O3–H3	110(2)

[a] Symmetry code: 1: $-x + 1$, y, $-z$. [b] Symmetry code: 1: $-x + 1$, y, $-z + 2$.

(98:70) $[NiL1 + H]^+$/$[NiL1 - H]^+$, 225/224 (65:45) $[HL1]^+$/$[HL1 - H]^+$, 179 (95) $[C_6H_4(CH{=}NH)ONi + H]^+$, 121 (30) $[CH(C_6H_5)(CH_3)(NH_2)]^+$, 105 (100) $[CH(C_6H_5)(CH_3)]^+$. $C_{60}H_{56}N_4O_4Ni_2(\mu\text{-}H_2O)\cdot 2CH_3OH$ (1096.65): calcd. C 67.91, H 6.07, N 5.11; found C 68.50, H 5.80, N 5.02.

μ-Aqua-tetrakis[(*R*)-*N*-1-(4-methoxyphenyl)ethylsalicylaldiminato]-di-Λ-nickel(II) (*R*-2): Yield 300 mg (75%). $[\alpha]^{25}$ (c = 0.05 g/100 mL, $CHCl_3$): + 350.9° (589 nm). MS (EI, 70 eV): m/z (%) = 566 (15) $[M]^+$, 313/311 (28:25) $[NiL2 + H]^+$/$[NiL2 - H]^+$, 255/254 (12:28) $[HL2]^+$/$[HL2 - H]^+$, 179 (15) $[C_6H_4(CH{=}NH)ONi + H]^+$, 135 (100) $[CH(CH_3)(C_6H_4OCH_3)]^+$, 105 (10) $[CH(C_6H_5)(CH_3)]^+$ (M = $C_{32}H_{32}N_2O_4Ni$, HL2 = $C_{16}H_{17}NO_2$). $C_{64}H_{64}N_4O_8Ni_2(\mu\text{-}H_2O)\cdot 2CH_3OH$ (1216.76): calcd. C 65.15, H 6.13, N 4.60; found C 64.26, H 5.92, N 4.56.

μ-Aqua-tetrakis[(*S*)-*N*-1-(4-methoxyphenyl)ethylsalicylaldiminato]-di-Λ-nickel(II) (*S*-2): Yield 315 mg (79%). $[\alpha]^{25}$ (c = 0.04 g/100 mL, $CHCl_3$): –357.1° (589 nm). MS (EI, 70 eV): m/z (%) = 566 (15) $[M]^+$, 313/311 (30:27) $[NiL2 + H]^+$/$[NiL2 - H]^+$, 255/254 (17:28) $[HL2]^+$/$[HL2 - H]^+$, 179 (15) $[C_6H_4(CH{=}NH)ONi + H]^+$, 135 (100) $[CH(CH_3)(C_6H_4OCH_3)]^+$, 105 (12) $[CH(C_6H_5)(CH_3)]^+$. $C_{64}H_{64}N_4O_8Ni_2(\mu\text{-}H_2O)\cdot 2H_2O$ (1188.70): calcd. C 64.67, H 5.94, N 4.71; found C 64.46, H 6.10, N 4.46.

μ-Aqua-tetrakis[(*R*)-*N*-1-(4-chlorophenyl)ethylsalicylaldiminato]di-Λ-nickel(II) (*R*-3): Yield 275 mg (70%). $[\alpha]^{25}$ (c = 0.06 g/100 mL,

Table 4. Crystal data and structure refinement for the complexes.

	R-**2**	*S*-**2**	*R*-**3**	*S*-**3**
Empirical formula	$C_{66}H_{74}N_4Ni_2O_{11}$	$C_{64}H_{66}N_4Ni_2O_{11}$[a]	$C_{62}H_{62}Cl_4N_4Ni_2O_7$	$C_{62}H_{62}Cl_4N_4Ni_2O_7$
M [g mol^{-1}]	1216.71	1184.63	1234.38	1234.38
Crystal size [mm^3]	0.51 × 0.46 × 0.44	0.91 × 0.81 × 0.74	0.57 × 0.25 × 0.14	0.55 × 0.35 × 0.29
θ range [°] (completeness)	1.62–25.12 (99.3%)	1.74–25.11 (99.7%)	1.66–25.15 (99.5%)	1.65–25.16 (99.3%)
h, k, l range	±29, ±11, ±15	±29, ±11, ±15	±29, ±11, ±15	±29, ±11, ±15
Crystal system	monoclinic	monoclinic	monoclinic	monoclinic
Space group	*C*2	*C*2	*C*2	*C*2
a [Å]	24.805(3)	24.780(3)	24.872(2)	24.880(3)
b [Å]	10.0274(11)	10.0095(11)	9.9002(10)	9.8905(11)
c [Å]	13.3043(13)	13.2503(14)	13.0192(13)	13.0306(15)
β [°]	108.965(7)	108.876(7)	109.092(5)	109.043(6)
V [Å^3]	3129.5(6)	3109.8(6)	3029.5(5)	3031.0(6)
$Z/D_{calcd.}$ [g cm^{-3}]	2/1.291	2/1.265	2/1.353	2/1.353
μ(Mo-K_α) [mm^{-1}]	0.663	0.666	0.852	0.852
F(000)	1284	1244	1284	1284
Max./min. transmission	0.7585/0.7271	0.6375/0.5813	0.8929/0.6441	0.7878/0.6516
Reflections collected	9047	8986	13532	13295
Independent reflns. (R_{int})	5020 (0.0153)	4603 (0.0193)	5387 (0.0206)	5372 (0.0183)
Data/restraints/parameters	5020/4/381	4603/2/372	5387/2/365	5372/2/365
Max./min. $\Delta\rho$ [e Å^{-3}][b]	0.316/–0.183	0.398/–0.202	0.368/–0.373	0.372/–0.373
$R1$/$wR2$ [$I > 2\sigma(I)$][c]	0.0371/0.0979	0.0422/0.1115	0.0301/0.0765	0.0277/0.0708
$R1$/$wR2$ (all data)[c]	0.0421/0.1026	0.0494/0.1186	0.0326/0.0785	0.0301/0.0724
Goodness-of-fit on F^2[d]	1.041	1.060	1.016	1.037
Flack parameter[e]	–0.028(16)	–0.034(18)	–0.010(11)	–0.002(11)

[a] Hydrogen atoms of crystal water molecule not found and not included in refinement. [b] Largest difference peak and hole. [c] $R1 = [\Sigma(||F_o| - |F_c||)/\Sigma|F_o|]$; $wR2 = \{\Sigma[w(F_o^2 - F_c^2)^2]/\Sigma[w(F_o^2)^2]\}^{1/2}$. [d] Goodness-of-fit = $\{\Sigma[w(F_o^2 - F_c^2)^2]/(n - p)\}^{1/2}$. [e] Absolute structure parameter.[26]

$CHCl_3$): + 367.5° (589 nm). MS (EI, 70 eV): *m/z* (%) = 632 (5) $[(NiL3 - H)_2]^+$, 576 (26) $[M]^+$, 317/315 (100:56) $[NiL3 + H]^+$/$[NiL3 - H]^+$, 259/258 (30:51) $[HL3]^+$/$[HL3 - H]^+$, 179 (95) $[C_6H_4(CH{=}NH)ONi + H]^+$, 139 (75) $[CH(CH_3)(C_6H_4Cl)]^+$, 121 (25) $[CH(C_6H_5)(CH_3)(NH_2)]^+$, 103 (45) $[C_6H_5(CN)]^+$ (M = $C_{30}H_{26}N_2O_2Cl_2Ni$, HL3 = $C_{15}H_{14}NOCl$). $C_{60}H_{52}N_4O_4Cl_4Ni_2(\mu\text{-}H_2O)\cdot 2CH_3OH$ (1234.45): calcd. C 60.33, H 5.06, N 4.54; found C 59.80, H 4.99, N 4.43.

μ-Aqua-tetrakis[(*S*)-*N*-1-(4-chlorophenyl)ethylsalicylaldiminato]di-Δ-nickel(II) (*S*-3): Yield 290 mg (74%). $[a]^{25}$ (*c* = 0.06 g/100 mL, $CHCl_3$): –375.0° (589 nm). MS (EI, 70 eV): *m/z* (%) = 632 (4) $[(NiL3 - H)_2]^+$, 576 (28) $[M]^+$, 317/315 (100:57) $[NiL3 + H]^+$/$[NiL3 - H]^+$, 259/258 (35:52) $[HL3]^+$/$[HL3 - H]^+$, 179 (90) $[C_6H_4(CH{=}NH)ONi + H]^+$, 139 (80) $[CH(CH_3)(C_6H_4Cl)]^+$, 121 (30) $[CH(C_6H_5)(CH_3)(NH_2)]^+$, 103 (50) $[C_6H_5(CN)]^+$. $C_{60}H_{52}N_4O_4Cl_4Ni_2\cdot 2CH_3OH$ (1234.45): calcd. C 60.33, H 5.06, N 4.54; found C 59.75, H 5.07, N 4.32.

μ$_2$-Aqua-tetrakis[(*R*)-*N*-1-(4-bromophenyl)ethylsalicylaldiminato]di-nickel(II) (*R*-4): Yield 300 mg (77%). $[a]^{25}$ (*c* = 0.07 g/100 mL, $CHCl_3$): + 392.9° (589 nm). MS (EI, 70 eV): *m/z* (%) = 722 (3) $[(NiL4 - H)_2]^+$, 664 (23) $[M]^+$, 363/361 (78:100) $[NiL4 + H]^+$/$[NiL4 - H]^+$, 303/302 (32:36) $[HL4]^+$/$[HL4 - H]^+$, 183 (64) $[CH(CH_3)(C_6H_4Br)]^+$, 179 (95) $[C_6H_4(CH{=}NH)ONi + H]^+$, 121 (50) $[CH(C_6H_5)(CH_3)(NH_2)]^+$, 104 (95) $[C_6H_5(CN) + H]^+$, 103 (22) $[C_6H_5(CN)]^+$ (M = $C_{30}H_{26}N_2O_2Br_2Ni$, HL4 = $C_{15}H_{14}NOBr$). $C_{60}H_{52}Br_4N_4O_4Ni_2\cdot H_2O\cdot 2CH_3OH$ (1412.28): calcd. C 52.73, H 4.43, N 3.97; found C 52.47, H 4.00, N 3.91.

X-ray Crystallography: Suitable single crystals were carefully selected under a polarizing microscope.

Data Collection: Bruker Kappa APEX2 CCD diffractometer (with microfocus tube) at 293 ± 2 K; Mo-K_α radiation (λ = 0.71073 Å), multilayer mirror system, ω scan; data collection with Apex2,[28] cell refinement and data reduction with SAINT,[29] experimental absorption correction with SADABS.[30]

Structure Analysis and Refinement: The structures were solved by direct methods using SHELXS-97; refinement was carried out by full-matrix least-squares methods on F^2 using the SHELXL-97 program suite.[27] All non-hydrogen atoms were refined with anisotropic displacement parameters. Hydrogen atoms for aromatic CH, aliphatic CH, and CH_3 groups were positioned geometrically (C–H 0.93 Å for aromatic CH, C–H 0.98 Å for aliphatic CH, C–H 0.96 Å for CH_3) and refined by using a riding model (AFIX 43 for aromatic CH, AFIX 13 for CH, AFIX 137 for CH_3) with U_{iso}(H) = 1.2U_{eq}(CH, CH_2) and U_{iso}(H) = 1.5U_{eq}(CH_3). For **2** and **3**, the symmetry-unique bridging aqua ligand hydrogen atom was found and refined by using U_{iso}(H) = 1.5U_{eq}(O). For *R*-**2**, the methanol (O)H atom was found, but had to kept fixed in subsequent refinements. For *S*-**2**, the hydrogen atoms of the crystal water molecule were neither found nor calculated and hence not refined. For *R*-**3** and *S*-**3**, the methanol (O)H atom was found and refined by using U_{iso}(H) = 1.5U_{eq}(O). The methyl group of the methoxy substituent of one nonbridging salicylaldiminato ligand in compounds *R*-**2** and *S*-**2** was disordered over two positions with 72:28 and 55:45 occupation, respectively, and refined by using the PART command. Details of the X-ray structure determinations and refinements are provided in Table 4. The graphics were drawn by using DIAMOND.[31]

CCDC-1058052 (for *S*-**2**), -1058053 (for *R*-**2**), -1058054 (for ***S*-3**), and -1058055 (for *R*-**3**) contain the supplementary crystallographic data for this paper. These data can be obtained free of charge from The Cambridge Crystallographic Data Centre via www.ccdc.cam.ac.uk/data_request/cif.

Computational Section: DFT calculations were carried out with the Gaussian 09[32] using default parameters and convergence criteria. The X-ray structure of compound **1** was employed as the input geometry, after optimization of the hydrogen atoms only, whereas

all other atoms were kept frozen. The B3LYP functional and TZVP basis set were employed in the calculations, which were performed in vacuo.

Acknowledgments

This work was supported by the Ministry of Science and Technology (MOST), Dhaka, Bangladesh (project number 2012/13). The authors thank the Alexander von Humboldt Foundation (AvH), Germany for offering a fellowship to M. E. Professor Prasad L. Polavarapu, Department of Chemistry, Vanderbilt University, Nashville, TN is sincerely thanked for many useful discussions.

[1] a) H. Amouri, M. Gruselle, *Chirality in Transition Metal Chemistry*, Wiley, Chichester, UK, **2008**; b) A. von Zelewsky, *Stereochemistry of Coordination Compounds*, Wiley, Chichester, UK, **1995**; c) U. Knof, A. von Zelewsky, *Angew. Chem. Int. Ed.* **1999**, *38*, 302–322; *Angew. Chem.* **1999**, *111*, 312.

[2] a) A. von Zelewsky, O. Mamula, *J. Chem. Soc., Dalton Trans.* **2000**, 219–231; b) P. J. Steel, *J. Organomet. Chem.* **1991**, *408*, 395–402; c) P. Hayoz, A. von Zelewsky, *Tetrahedron Lett.* **1992**, *33*, 5165–5168; d) R. Vadavi, E. D. Conrad, D. I. Arbuckle, T. S. Cameron, E. Essoun, M. A. S. Aquino, *Inorg. Chem.* **2011**, *50*, 11862–11864; e) B. R. Groves, D. I. Arbuckle, E. Essoun, T. L. Lundrigan, R. Wang, M. A. S. Aquino, *Inorg. Chem.* **2013**, *52*, 11563–11572; f) L. J. Boudreau, T. L. Clarke, A. H. Murray, K. N. Robertson, T. S. Cameron, M. A. S. Aquinoa, *Inorg. Chim. Acta* **2013**, *394*, 152–158.

[3] a) E. C. Constable, G. Zhang, C. E. Housecroft, M. Neuburger, J. A. Zampese, *Chem. Commun.* **2010**, 3077–3079; b) E. C. Constable, C. E. Housecroft, T. Kulke, C. Lazzarini, E. R. Schofield, Y. Zimmermann, *J. Chem. Soc., Dalton Trans.* **2001**, 2864–2871; c) S. Sprouse, K. A. King, P. J. Spellane, R. J. Watts, *J. Am. Chem. Soc.* **1984**, *106*, 6647–6653; d) U. Mäder, T. Jenny, A. van Zelewsky, *Helv. Chim. Acta* **1986**, *69*, 1085–1087.

[4] a) K. Warnmark, J. A. Thomas, O. Heyke, J.-M. Lehn, *Chem. Commun.* **1996**, 701–702; b) F. M. MacDonnell, S. Bodige, *Inorg. Chem.* **1996**, *35*, 5758–5759; c) S. Bodige, A. S. Torres, D. J. Maloney, D. Tale, G. R. Kinsel, A. K. Walker, F. M. MacDonnell, *J. Am. Chem. Soc.* **1997**, *119*, 10364–10369; d) K. Wärnmark, O. Heyke, J. A. Thomas, J.-M. Lehn, *Chem. Commun.* **1996**, 2603–2604; e) T. J. Rutherford, M. G. Quagliotto, F. R. Keene, *Inorg. Chem.* **1995**, *34*, 3857–3858; f) D. Tzalis, Y. Tor, *J. Am. Chem. Soc.* **1997**, *119*, 852–853.

[5] a) E. Emst, M. J. O'Connor, R. H. Holm, *J. Am. Chem. Soc.* **1967**, *89*, 6104–6113; b) H. Okawa, M. Nakamura, S. Kida, *Inorg. Chim. Acta* **1986**, *120*, 185–189; c) R. S. Downing, F. L. Urbach, *J. Am. Chem. Soc.* **1969**, *91*, 5977–5983; d) B. Bosnich, *J. Am. Chem. Soc.* **1968**, *90*, 627–632.

[6] a) T. Akitsu, Y. Einaga, *Polyhedron* **2005**, *24*, 2933–2943; b) T. Akitsu, Y. Einaga, *Acta Crystallogr., Sect. C* **2004**, *60*, m640–m642; c) H. Sakiyama, H. Okawa, N. Matsumoto, S. Kida, *J. Chem. Soc., Dalton Trans.* **1990**, 2935–2939; d) G.-P. Li, Q.-C. Yang, Y.-Q. Tang, Y.-D. Guan, Z.-H. Shang, *Acta Chim. Sinica* **1987**, *45*, 421–425.

[7] a) C. Evans, D. Luneau, *J. Chem. Soc., Dalton Trans.* **2002**, 83–86; b) H. Sakiyama, H. Okawa, N. Matsumoto, S. Kida, *Bull. Chem. Soc. Jpn.* **1991**, *64*, 2644–2647; c) T. Akitsu, *Polyhedron* **2007**, *26*, 2527–2535; d) T. Akitsu, Y. Einaga, *Polyhedron* **2005**, *24*, 1869–1877.

[8] F. Wang, H. Zhang, L. Li, H.-Q. Hao, X.-Y. Wang, J.-G. Chen, *Tetrahedron: Asymmetry* **2006**, *17*, 2059–2063.

[9] A.-C. Chamayou, S. Lüdeke, V. Brecht, T. B. Freedman, L. A. Nafie, C. Janiak, *Inorg. Chem.* **2011**, *50*, 11363–11374.

[10] a) E. C. Constable, C. E. Housecroft, V. Jullien, M. Neuburger, I. Poleschak, S. Reymann, S. Saxer, S. Schaffner, *Polyhedron* **2007**, *26*, 5519–5526; b) E. C. Constable, *Chem. Soc. Rev.* **2013**, *42*, 1637–1651.

[11] a) H. S. Chow, E. C. Constable, R. Frantz, C. E. Housecroft, J. Lacour, M. Neuburger, D. Rappoport, S. Schaffner, *New J. Chem.* **2009**, *33*, 376–385; b) G. Brewer, C. Brewer, R. J. Butcher, G. T. Robichaux, C. Viragh, *Inorg. Chim. Acta* **2014**, *410*, 171–177.

[12] M. Enamullah, A. K. M Royhan Uddin, G. Pescitelli, R. Berardozzi, G. Makhloufi, V. Vasylyeva, A.-C. Chamayou, C. Janiak, *Dalton Trans.* **2014**, *43*, 3313–3329.

[13] M. Enamullah, M. A. Quddus, G. Pescitelli, R. Berardozzi, G. Makhloufi, C. Janiak, *unpublished results.*

[14] M. Enamullah, V. Vasylyeva, C. Janiak, *Inorg. Chim. Acta* **2013**, *408*, 109–119.

[15] M. Enamullah, M. K. Islam, *J. Coord. Chem.* **2013**, *66*, 4107–4118.

[16] a) A. P. Smirnoff, *Helv. Chim. Acta* **1920**, *3*, 177–195; b) U. Mäder, A. von Zelewsky, H. Stoeckli-Evans, *Helv. Chim. Acta* **1992**, *75*, 1320–1332.

[17] a) L. Ghizdavu, B. Kolp, A. von Zelewsky, H. Stoeckli-Evans, *Eur. J. Inorg. Chem.* **1999**, 1271–1279; b) M. Gianini, A. Forster, P. Haag, A. von Zelewsky, H. Stoeckli-Evans, *Inorg. Chem.* **1996**, *35*, 4889–4895; c) L. R. Guez, E. Labisbal, A. S. Pedrares, J. A. Garcia-Vazquez, J. Romero, M. L. Duran, J. A. Real, A. Sousa, *Inorg. Chem.* **2006**, *45*, 7903–7914.

[18] M. Enamullah, M. A. Quddus, M. A. Halim, M. K. Islam, V. Vasylyeva, C. Janiak, *Inorg. Chim. Acta* **2015**, *427*, 103–111.

[19] a) E. D. Mckenzie, F. S. Stephens, *Inorg. Chim. Acta* **1979**, *32*, 253–261; b) E. D. Mckenzie, F. S. Stephens, *Inorg. Chim. Acta* **1978**, *26*, L49–L50.

[20] M. Enamullah, A. K. M. Royhan Uddin, A.-C. Chamayou, C. Janiak, *Z. Naturforsch. B* **2007**, *62*, 807–817.

[21] C. Janiak, A.-C. Chamayou, A. K. M. Royhan Uddin, M. Uddin, K. S. Hagen, M. Enamullah, *Dalton Trans.* **2009**, 3698–3709.

[22] M. Enamullah, A. K. M. Royhan Uddin, G. Hogarth, C. Janiak, *Inorg. Chim. Acta* **2012**, *387*, 173–180.

[23] a) M. Enamullah, A. Sharmin, M. Hasegawa, T. Hoshi, A.-C. Chamayou, C. Janiak, *Eur. J. Inorg. Chem.* **2006**, 2146–2154; b) M. Enamullah, *J. Coord. Chem.* **2011**, *64*, 1608–1616; c) M. Enamullah, *J. Coord. Chem.* **2012**, *65*, 911–922; d) M. Enamullah, A. K. M. Royhan Uddin, G. Hogarth, *J. Coord. Chem.* **2012**, *65*, 4263–4276.

[24] a) B.-H. Ye, I. D. Williams, X.-Y. Li, *J. Inorg. Biochem.* **2002**, *92*, 128–136; b) D. Lin-Vien, N. B. Colthup, W. G. Fateley, J. G. Grasselli, *The Handbook of Infrared and Raman Characteristic Frequencies of Organic Molecules*, Academic Press, California, **1991**, p. 46.

[25] a) M. Enamullah, A. K. M. Royhan Uddin, *J. Bangladesh Chem. Soc.* **2009**, *22*, 44–54; b) M. Enamullah, F. Renz, U. El-Ayaan, G. Wiesinger, W. Linert, *Vib. Spectrosc.* **1997**, *14*, 95–104; c) M. Enamullah, W. Linert, *J. Coord. Chem.* **1996**, *40*, 193–201; d) M. Enamullah, W. Linert, V. Gutmann, R. F. Jameson, *Monatsh. Chem.* **1994**, *125*, 661–670; e) M. Enamullah, W. Linert, V. Gutmann, *Vib. Spectrosc.* **1995**, *9*, 265–271; f) M. Enamullah, W. Linert, *J. Coord. Chem.* **1995**, *35*, 325–335; g) M. Enamullah, W. Linert, *J. Coord. Chem.* **1996**, *38*, 337–346.

[26] a) H. D. Flack, *Acta Crystallogr., Sect. A* **1983**, *39*, 876–881; b) H. D. Flack, G. Bernardinelli, *Acta Crystallogr., Sect. A* **1999**, *55*, 908–915; c) H. D. Flack, G. Bernardinelli, *Chirality* **2008**, *20*, 681–690; d) H. D. Flack, M. Sadki, A. L. Thompson, D. J. Watkin, *Acta Crystallogr., Sect. A* **2011**, *67*, 21–34.

[27] G. M. Sheldrick, *Acta Crystallogr., Sect. A* **2008**, *64*, 112–122.

[28] *Apex2*, *Data Collection Program for the CCD Area-Detector System*, Bruker Analytical X-ray Systems, Madison, WI, **1997–2006**.

[29] *SAINT, data reduction and frame integration program for the CCD area-detector system*, Bruker Analytical X-ray Systems, Madison, WI, **2006**.

[30] G. Sheldrick, *SADABS: Area-detector absorption correction*, University of Göttingen, Germany, **1996**.
[31] K. Brandenburg, *DIAMOND* (version 3.2), *Crystal and Molecular Structure Visualization, Crystal Impact*, K. Brandenburg & H. Putz Gbr, Bonn, Germany, **2009**.
[32] M. J. Frisch, G. W. Trucks, H. B. Schlegel, G. E. Scuseria, M. A. Robb, J. R. Cheeseman, G. Scalmani, V. Barone, B. Mennucci, G. A. Petersson, H. Nakatsuji, M. Caricato, X. Li, H. P. Hratchian, A. F. Izmaylov, J. Bloino, G. Zheng, J. L. Sonnenberg, M. Hada, M. Ehara, K. Toyota, R. Fukuda, J. Hasegawa, M. Ishida, T. Nakajima, Y. Honda, O. Kitao, H. Nakai, T. Vreven, J. A. Montgomery, J. E. Peralta, F. Ogliaro, M. Bearpark, J. J. Heyd, E. Brothers, K. N. Kudin, V. N. Staroverov, R. Kobayashi, J. Normand, K. Raghavachari, A. Rendell, J. C. Burant, S. S. Iyengar, J. Tomasi, M. Cossi, N. Rega, J. M. Millam, M. Klene, J. E. Knox, J. B. Cross, V. Bakken, C. Adamo, J. Jaramillo, R. Gomperts, R. E. Stratmann, O. Yazyev, A. J. Austin, R. Cammi, C. Pomelli, J. W. Ochterski, R. L. Martin, K. Morokuma, V. G. Zakrzewski, G. A. Voth, P. Salvador, J. J. Dannenberg, S. Dapprich, A. D. Daniels, Farkas, J. B. Foresman, J. V. Ortiz, J. Cioslowski, D. J. Fox, *Gaussian 09*, Revision C.01, Wallingford, CT, **2009**.

Received: April 9, 2015
Published Online: May 11, 2015

